

Lattice calculation of the pion mass difference $M_{\pi^+} - M_{\pi^0}$ at order $\mathcal{O}(\alpha_{\text{em}})$

R. Frezzotti^{1,*} G. Gagliardi^{2,†} V. Lubicz^{3,‡} G. Martinelli^{4,§} F. Sanfilippo^{2,||} and S. Simula^{2,¶}

¹*Dipartimento di Fisica and INFN, Università di Roma Tor Vergata,*

Via della Ricerca Scientifica 1, I-00133 Rome, Italy

²*Istituto Nazionale di Fisica Nucleare, Sezione di Roma Tre,*

Via della Vasca Navale 84, I-00146 Rome, Italy

³*Dipartimento di Matematica e Fisica, Università Roma Tre and INFN,*

Sezione di Roma Tre, Via della Vasca Navale 84, I-00146 Rome, Italy

⁴*Dipartimento di Fisica and INFN Sezione di Roma La Sapienza,*

Piazzale Aldo Moro 5, I-00185 Rome, Italy



(Received 7 March 2022; accepted 3 June 2022; published 8 July 2022)

We present a lattice calculation of the charged/neutral pion mass difference $M_{\pi^+} - M_{\pi^0}$ at order $\mathcal{O}(\alpha_{\text{em}})$ using the gauge configurations produced by the Extended Twisted Mass Collaboration with $N_f = 2 + 1 + 1$ dynamical quark flavors at three values of the lattice spacing ($a \simeq 0.062, 0.082, 0.089$ fm) and pion masses in the range $M_\pi \simeq 250\text{--}500$ MeV. We employ the RM123 method and expand the path integral around the isospin symmetric point at leading order in the electromagnetic coupling α_{em} . Making use of the recently proposed *rotated twisted-mass* scheme, we evaluate the full $\mathcal{O}(\alpha_{\text{em}})$ contribution, with the inclusion of the disconnected diagram. At the physical point, after performing the continuum and infinite volume extrapolation, we obtain the value $M_{\pi^+} - M_{\pi^0} = 4.622(95)$ MeV which is in good agreement with the experimental result $[M_{\pi^+} - M_{\pi^0}]^{\text{exp}} = 4.5936(5)$ MeV.

DOI: [10.1103/PhysRevD.106.014502](https://doi.org/10.1103/PhysRevD.106.014502)

I. INTRODUCTION

In the last decade, the precision achieved in the computation of several observables relevant for flavor physics by lattice QCD has reached a level where electromagnetic and strong isospin-breaking (IB) effects can no longer be neglected [1]. The issue of how to evaluate QED effects from lattice QCD simulations has been addressed so far in two different ways: the first method (see e.g., Refs. [2–5]) consists in including QED to the action, performing QCD + QED simulations at different values of the electromagnetic coupling α_{em} and extrapolating to the physical value. The second method, the so-called RM123 method [6–13], consists in expanding the path integral around the isospin symmetric point $m_d = m_u$, in powers of the small parameters α_{em} and $m_d - m_u$, with $\alpha_{\text{em}} \sim (m_d - m_u)/\Lambda_{\text{QCD}} \sim \mathcal{O}(10^{-2})$.

This approach allows to express the expectation value of any given observable in QCD + QED as a power series in α_{em} and $m_d - m_u$ whose coefficients are related to correlation functions evaluated in the isospin symmetric theory. This has also the advantage that only standard lattice QCD simulations needs to be performed.

In the last years, the RM123 method has been successfully applied to the computation of the leading electromagnetic and IB effects to the hadron spectrum, as in the case of the charged/neutral mass splitting of light, strange and charmed pseudoscalar mesons [7, 14]. In the case of the neutral pion mass M_{π^0} , its diagrammatic expansion contains a quark-line disconnected diagram connected by a photon line [see Eq. (8)], in the following simply called “disconnected diagram,” which contributes to the charged/neutral pion mass difference $M_{\pi^+} - M_{\pi^0}$. Computing such diagram is a highly nontrivial numerical problem, and moreover, it can be shown that, as a consequence of the Dashen theorem [15], this disconnected diagram represents a tiny contribution of order $\mathcal{O}(\alpha_{\text{em}} \hat{m}_\ell)$. For this reason it has been neglected in our previous study [14]. The aim of this paper is to evaluate both the connected and disconnected contributions entering $M_{\pi^+} - M_{\pi^0}$ at order $\mathcal{O}(\alpha_{\text{em}})$.

For this calculation, we use the *rotated twisted-mass* (RTM) scheme introduced in Ref. [16]. We have recently shown that this method is particularly convenient for IB and QED calculations based on the RM123 approach, since it allows us to consider correlation functions which are

*roberto.frezzotti@roma2.infn.it

†giuseppe.gagliardi@roma3.infn.it

‡vittorio.lubicz@uniroma3.it

§guido.martinelli@roma1.infn.it

||francesco.sanfilippo@infn.it

¶silvano.simula@roma3.infn.it

Published by the American Physical Society under the terms of the [Creative Commons Attribution 4.0 International license](https://creativecommons.org/licenses/by/4.0/). Further distribution of this work must maintain attribution to the author(s) and the published article’s title, journal citation, and DOI. Funded by SCOAP³.

affected by much smaller statistical fluctuations with respect to the ones appearing in the RM123 expansion with standard twisted mass (TM) fermions. Evaluating the disconnected diagram appearing in the charged/neutral pion mass difference using the RTM scheme provides in turn an ideal benchmark test in view of its applications to more complicated cases such as the evaluation of the disconnected diagrams relevant for the semileptonic pion and kaon decay (π_{ℓ_3}, K_{ℓ_3}).

For the numerical simulations, we use the pure QCD isospin symmetric gauge ensembles generated by the Extended Twisted Mass Collaboration (ETMC) with $N_f = 2 + 1 + 1$ dynamical quarks [17,18]. With respect to our previous analysis [14], we perform simulations on larger lattice volumes, using two additional ensembles with linear lattice extent $L \sim 3.5$ and 4.2 fm and lattice spacing $a \sim 0.089$ fm, and adopt an improved ansatz in the extrapolation to the physical pion mass and to the continuum and infinite volume limit. Our final result is

$$M_{\pi^+} - M_{\pi^0} = 4.622(64)_{\text{stat}}(70)_{\text{sys}} \text{ MeV}, \quad (1)$$

in very good agreement with the experimental value [19]

$$[M_{\pi^+} - M_{\pi^0}]^{\text{exp}} = 4.5936(5) \text{ MeV}. \quad (2)$$

The paper is organized as follows: in Sec. II we present our lattice setup and a recap of the RM123 method, focusing on the evaluation of the pion mass splitting in the standard basis and in the RTM scheme. In Sec. III we present our numerical results for $M_{\pi^+} - M_{\pi^0}$, computed in the RTM scheme with the inclusion of the disconnected diagram. Finally, in Sec. IV we draw our conclusions.

II. METHODOLOGY

A. Lattice discretization of isospin symmetric QCD

We use the QCD isospin symmetric gauge configurations produced by the ETMC and generated with the maximally twisted Wilson action for fermions, and the Iwasaki action for gluons. All details concerning the lattice discretization have been already presented elsewhere [18]. The fermionic action describes $N_f = 2 + 1 + 1$ quark flavors which include in the sea, besides two mass-degenerate quarks, also the strange and charm quarks with masses close to their physical values. The untwisted bare quark mass is tuned to its critical value, which guarantees the automatic $\mathcal{O}(a)$ improvement of parity-even observables [20]. We consider three values of the inverse bare lattice coupling β as well as different lattice sizes. For each lattice spacing, several values of the light sea quark mass are considered in order to perform a reliable extrapolation to its physical value. The complete list of lattice ensembles along with the values of the bare quark masses we use and the number of gauge configurations N_{cfg} accumulated for each ensemble is collected in Table I.

B. QED and strong IB corrections: The standard RM123 approach

The leading electromagnetic and strong IB corrections are evaluated adopting the RM123 method [7,14]. The starting point is the compact formulation of QED on the lattice in which the photon field $A_\mu(x)$ is introduced in the pure QCD lattice action through the replacement

TABLE I. Details of the lattice ensembles we use for the present study. They have been generated by the ETMC employing $N_f = 2 + 1 + 1$ dynamical quark flavors, with degenerate u and d quark masses [17,18], and correspond to lattice spacings in the range $a \in [0.062, 0.089]$ fm and pion masses $M_\pi \in [250, 500]$ MeV. For each ensemble we also quote the total number N_{cfg} of accumulated independent gauge configurations.

Ensemble	β	a^{-1} (GeV)	V/a^4	M_π (MeV)	$M_\pi L$	$a\mu_{\text{sea}} = a\mu_{\text{val}}$	N_{cfg}
A30.32	1.90	2.227 (85)	$32^3 \times 64$	275 (10)	3.95	0.0030	150
A40.32				316 (12)	4.54	0.0040	100
A50.32				350 (13)	5.03	0.0050	150
A40.24			$24^3 \times 48$	322 (13)	3.40	0.0040	150
A60.24				386 (15)	4.18	0.0060	150
A80.24				442 (17)	4.77	0.0080	150
A100.24				495 (19)	5.34	0.0100	150
A40.40			$40^3 \times 80$	317 (12)	5.69	0.0040	150
A40.48			$48^3 \times 96$	316 (12)	6.80	0.0040	100
B35.32	1.95	2.418 (84)	$32^3 \times 64$	302 (10)	3.98	0.0035	150
B55.32				375 (13)	4.96	0.0055	150
B75.32				436 (15)	5.76	0.0075	80
B85.24			$24^3 \times 48$	468 (16)	4.64	0.0085	150
D20.48	2.10	3.187 (81)	$48^3 \times 96$	255 (7)	3.84	0.0020	100
D30.48				318 (8)	4.69	0.0030	100

$$\begin{aligned}\nabla_\mu \psi_f(x) &= U_\mu(x) \psi_f(x + a\hat{\mu}) - \psi_f(x) \\ &\rightarrow e^{ieq_f A_\mu(x)} U_\mu(x) \psi_f(x + a\hat{\mu}) - \psi_f(x),\end{aligned}\quad (3)$$

together with the inclusion of the pure gauge photon action $S_{\text{gauge}}[A_\mu]$ in Feynman gauge

$$\begin{aligned}S_{\text{gauge}}[A_\mu] &= \frac{1}{2} \sum_{x,\mu,\nu} A_\mu(x) [-\nabla_\nu^* \nabla_\nu] A_\mu(x) \\ &= \frac{1}{2} \sum_{k,\mu,\nu} A_\mu^*(k) \left[2 \sin\left(\frac{k_\nu}{2}\right) \right]^2 A_\mu(k).\end{aligned}\quad (4)$$

In Eq. (3), $e^2 = 4\pi\alpha_{\text{em}}$, while q_f is the electric charge of the quark f in units of the electric charge of the positron. To cope with the infrared divergence of the photon propagator, we adopt the QED_L regularization and set $A_\mu(k_0, \vec{k} = 0) = 0$ for all k_0 . The resulting path integral is then expanded around the isospin symmetric point to the order $\mathcal{O}(\alpha_{\text{em}}, \hat{m}_d - \hat{m}_u)$, where $\hat{m}_{u/d}$ are the renormalized masses of the up and down quark in QCD + QED. It should be noted, that the presence of QED interactions produce additional ultraviolet divergences which are then absorbed through a set of properly defined counterterms [7].

At leading order in the IB parameters $(m_d - m_u)/\Lambda_{\text{QCD}} \sim \alpha_{\text{em}}$, the charged/neutral pion mass splitting is a

pure electromagnetic effect, since the leading IB corrections proportional to $m_d - m_u$ cancel out in both the charged and neutral pion correlators which are symmetric with respect to the exchange $u \leftrightarrow d$. Away from the isospin symmetric limit, the neutral pion mixes with the η and η' mesons [21]. However, such mixing, which is an $\mathcal{O}(m_d - m_u)$ effect, enters the neutral pion correlator only at the next-to-leading order, and for this reason, contaminations from the η and η' mesons are absent in our leading order calculation of the neutral pion correlator. According to the analysis of Ref. [7], at order $\mathcal{O}(\alpha_{\text{em}})$ the charged/neutral pion mass difference $M_{\pi^+} - M_{\pi^0}$ is given by

$$M_{\pi^+} - M_{\pi^0} = \frac{e^2}{2} (q_u - q_d)^2 \partial_t \frac{\delta C_\pi^{\text{exch}}(t) - \delta C_\pi^{\text{disc}}(t)}{C_{\pi\pi}(t)},\quad (5)$$

where $C_{\pi\pi}(t)$ is the pion correlator of isospin symmetric QCD, while the quantities $\delta C_\pi^{\text{exch}}(t)$ and $\delta C_\pi^{\text{disc}}(t)$ are defined in terms of the pion correlators of the isospin symmetric theory with two integrated insertions of the electromagnetic current $J_\mu(x)$, for which we consider here its local version¹

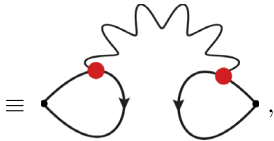
$$J_\mu(x) = e \sum_f q_f \bar{\psi}_f(x) \gamma_\mu \psi_f(x).\quad (6)$$

Explicitly one has²

$$\begin{aligned}\frac{e^2}{2} (q_u - q_d)^2 \delta C_\pi^{\text{exch.}}(t) &= -\frac{1}{\sqrt{L^3}} \sum_{\vec{x}, y, y'} \left[\langle 0 | T \left\{ \phi_{\pi^+}(\vec{x}, t) J_\mu(y) J_\nu(y') \phi_{\pi^+}^\dagger(0) \right\} | 0 \rangle \Delta_{\mu\nu}(y - y') - (\phi_{\pi^+} \rightarrow \phi_{\pi^0}) \right] \\ \Rightarrow \delta C_\pi^{\text{exch.}}(t) &= \frac{1}{\sqrt{L^3}} \sum_{\vec{x}, y, y'} \langle \text{Tr} \left[S_\ell((\vec{x}, t), y) \gamma_\mu S(y, 0) \gamma_5 S_\ell(0, y') \gamma_\nu S_\ell(y', (\vec{x}, t)) \gamma_5 \right] \rangle_U \Delta_{\mu,\nu}(y - y')\end{aligned}\quad (7)$$



$$\begin{aligned}\frac{e^2}{2} (q_u - q_d)^2 \delta C_\pi^{\text{disc.}}(t) &= -\frac{1}{\sqrt{L^3}} \sum_{\vec{x}, y, y'} \langle 0 | T \left\{ \phi_{\pi^0}(\vec{x}, t) J_\mu(y) J_\nu(y') \phi_{\pi^0}^\dagger(0) \right\} | 0 \rangle \Delta_{\mu\nu}(y - y') \\ \Rightarrow \delta C_\pi^{\text{disc.}}(t) &= \frac{1}{\sqrt{L^3}} \sum_{\vec{x}, y, y'} \langle \text{Tr} \left[S_\ell((\vec{x}, t), y) \gamma_\mu S(y, (\vec{x}, t)) \gamma_5 \right] \cdot \text{Tr} \left[S_\ell(0, y') \gamma_\nu S(y', 0) \gamma_5 \right] \rangle_U \Delta_{\mu,\nu}(y - y')\end{aligned}\quad (8)$$



¹The use of the (renormalized) local vector current in place of the exactly conserved point-split current adopted in our previous work [14] gives identical results up to $\mathcal{O}(a^2)$ lattice artifacts.

²The quark-line connected and disconnected Wick contractions have a relative minus sign stemming from the extra fermion loop present in the disconnected contribution. For convenience, we decided to pull out this extra minus sign from the definition of the disconnected diagram.

where L is the spatial lattice extent, $\Delta_{\mu\nu}$ is the photon propagator in Feynman gauge, $\langle 0| \cdot |0\rangle$ is the vacuum expectation value (VEV) computed in the isospin symmetric theory, and $\langle \cdot \rangle_U$ indicates the average over the SU(3) gauge field after integrating over the fermionic fields. $S_\ell(x, y)$ is the light quark propagator of isospin symmetric QCD, and the trace Tr is intended over color and Dirac indices. ϕ_{π^+} and ϕ_{π^0} are interpolating operators having the same quantum numbers of the positively charged and neutral pion, for which we choose

$$\phi_{\pi^+}(x) = i\bar{\psi}_d(x)\gamma_5\psi_u(x), \quad (9)$$

$$\phi_{\pi^0}(x) = i\frac{\bar{\psi}_u(x)\gamma_5\psi_u(x) - \bar{\psi}_d(x)\gamma_5\psi_d(x)}{\sqrt{2}}. \quad (10)$$

Following the definition given in Ref. [7], the operator $-\partial_t$ in Eq. (5) corresponds to the evaluation of the so-called effective slope $\delta m_{\text{eff}}(t)$ from the ratio of correlators $\delta C/C$, which is defined through

$$\begin{aligned} \delta m_{\text{eff}}(t) &\equiv -\partial_t \frac{\delta C(t)}{C(t)} \\ &= \frac{1}{F(T/2 - t, M)} \left(\frac{\delta C(t)}{C(t)} - \frac{\delta C(t-a)}{C(t-a)} \right), \end{aligned} \quad (11)$$

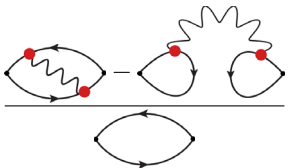
where in our case

$$\delta C(t) \equiv \delta C_\pi^{\text{exch}}(t) - \delta C_\pi^{\text{disc}}(t), \quad C(t) \equiv C_{\pi\pi}(t). \quad (12)$$

In Eq. (11), M is the ground state mass extracted from the correlator $C(t)$, T is the temporal extent of the lattice and the factor $F(x, M)$ is given by

$$F(x, M) = x \tanh(Mx) - (x+a) \tanh(M(x+a)). \quad (13)$$

In the large time limit $t \gg a$, $T-t \gg a$, where the ground state is dominant, the effective slope $\delta m_{\text{eff}}(t)$ tends to $M_{\pi^+} - M_{\pi^0}$. Making use of the previous definitions, we thus simply have

$$M_{\pi^+} - M_{\pi^0} = \frac{e^2}{2} (q_u - q_d)^2 \partial_t \frac{\text{Diagram}}{\text{Diagram}}, \quad (14)$$


where the diagram in the denominator of the right-hand side (rhs) is the pion correlator in isospin symmetric QCD. The result of Eq. (14) holds true also in the full unquenched theory. As argued in Ref. [7], the disconnected diagram $\delta C_\pi^{\text{disc}}$ vanishes in the SU(2) chiral limit as a consequence of the Dashen theorem: in the continuum limit, even in the presence of e.m. interactions, the neutral pion is an exact

Goldstone boson for $m_u = m_d = 0$ and arbitrary values of q_u and q_d since the electromagnetic current is diagonal in flavor space and it is invariant under a chiral transformation with generator τ_3 . This in particular implies (see Ref. [7] for details) that the disconnected contribution is of order $\mathcal{O}(\alpha_{\text{em}} m_\ell)$, and represents therefore a tiny corrections which has been neglected in the pioneering analysis of Ref. [7] and in the updated study which made use of $N_f = 2 + 1 + 1$ ensembles of Ref. [14]. However, aiming to a precise quantitative estimate of the $M_{\pi^+} - M_{\pi^0}$ mass difference, it is important to evaluate also the disconnected contribution, which is the main motivation for the present work. In addition, the computation of the disconnected diagram entering the pion mass splitting can be considered as a benchmark test in view of the computation of the disconnected diagrams appearing in, e.g., $K_{\ell 3}$ decays.

C. The charged/neutral pion mass difference in the RTM scheme

In the TM regularization of the lattice fermionic action, isospin is broken at finite lattice spacing already at the level of pure QCD. In particular, the neutral pion correlator involves disconnected diagrams, which cancel in the continuum due to isospin symmetry. Moreover, the related mass suffers from $\mathcal{O}(a^2 \Lambda_{\text{QCD}})$ cutoff effects. On the contrary, the charged pion correlator involves only connected diagram, and its mass is affected only by $\mathcal{O}(a^2 m_l)$ cut-off effects, behaving as a true Goldstone boson as shown in Refs. [20,22]. In addition, correlation functions involving the propagation of the TM neutral pion, are typically noisier than the corresponding charged ones. Therefore, the disconnected contribution to $M_{\pi^+} - M_{\pi^0}$ is very difficult to determine in the standard TM approach, due to the presence of large statistical fluctuations in the neutral sector.

In our previous analysis of the pion mass splitting [7,14], we evaluated Eq. (7) in a mixed action setup. In the valence sector, for each light quark flavor f , a pair of Osterwalder-Seiler fermions ψ_f^+ , ψ_f^- , having the same mass of the corresponding sea quark, but regularized with opposite values of the Wilson parameter, $r = \pm 1$, has been introduced. This allowed to compute the correlation functions in Eq. (7) using as interpolating field of the neutral and charged pion:

$$\phi_{\pi^+}(x) = i\bar{\psi}_d^-(x)\gamma_5\psi_u^+(x), \quad (15)$$

$$\phi_{\pi^0}(x) = i\frac{\bar{\psi}_u^+(x)\gamma_5\psi_u^-(x) - \bar{\psi}_d^-(x)\gamma_5\psi_d^-(x)}{\sqrt{2}}. \quad (16)$$

In this way both charged and neutral pions contain valence quarks carrying different signs of the twisted Wilson term. This choice gives rise to correlators having reduced statistical errors compared to other choices of

the interpolator fields like $\bar{\psi}_f^+ \psi_f^+$. However, within this mixed action setup, only the connected fermionic Wick contraction in Eq. (7) is non-zero, and in the continuum limit the corresponding correlation function only reproduces the correct contribution of $\delta C_\pi^{\text{exch}}$ to the pion mass splitting. In Refs. [7,14], the more noisy contribution $\delta C_\pi^{\text{disc}}(t)$ has been neglected.

In a recent paper [16], we showed that it is possible to evaluate both the exchange and disconnected diagrams by considering only correlation functions involving quark lines with opposite values of the Wilson parameter by working in the so-called RTM scheme. In this scheme, the pure isoQCD action of the light-quark sector is given by [16]

$$\mathcal{L}_{\text{RTM}}(\psi'_\ell) = \bar{\psi}'_\ell(x) [\gamma_\mu \tilde{\nabla}_\mu - i\gamma_5 \tau_3 W(m_{\text{cr}}) + \hat{m}_\ell] \psi'_\ell(x), \quad (17)$$

where $\psi'_\ell = (u', d')$, while $\tilde{\nabla}_\mu$ is the lattice symmetric covariant derivative, written in terms of the forward (∇_μ) and backward (∇_μ^*) covariant derivatives,

$$\tilde{\nabla}_\mu = \frac{1}{2} (\nabla_\mu^* + \nabla_\mu). \quad (18)$$

In Eq. (17), $W(m_{\text{cr}})$ is the critical Wilson term, which includes the critical mass m_{cr} , and it is given by

$$W(m_{\text{cr}}) = -a \frac{r}{2} \nabla_\mu \nabla_\mu^* + m_{\text{cr}}(r). \quad (19)$$

In the RTM scheme, the primed quark fields u' , d' are regularized with opposite values of the Wilson parameter $r = \pm 1$, and are related to the “physical” basis up and down quark fields, u , d , through the rotation

$$\begin{pmatrix} u' \\ d' \end{pmatrix} = \frac{1}{\sqrt{2}} \begin{pmatrix} 1 & 1 \\ -1 & 1 \end{pmatrix} \begin{pmatrix} u \\ d \end{pmatrix}. \quad (20)$$

Notice that the RTM action is not equivalent to the standard TM action, because the transformation in Eq. (20) does not correspond to a symmetry of the discretized theory due to the presence of the twisted Wilson term proportional to τ_3 . We call here “physical” quark basis the one where the isospin breaking terms proportional to $(m_u - m_d)/2$ and $(q_u - q_d)/2 = \Delta q$, once written in terms of $\psi'_\ell = (u, d)^T$, involve a τ_3 matrix. In the primed basis of Eq. (17) these isospin violating terms, expressed via the fields $\psi'_\ell = (u', d')^T$, involve instead a τ_1 matrix. The peculiarity of the RTM valence fermion action is that different Pauli matrices (e.g., τ_3 and τ_1) appear in the chirally twisted Wilson term and in the isospin breaking terms, whatever basis is taken.

In the basis of Eq. (17), the “rotated charged” pion fields $\phi_{\pi^-} = \bar{u}' \gamma_5 d'$ and $\phi_{\pi^+} = \bar{d}' \gamma_5 u'$ are related to the physical pion fields through

$$\begin{aligned} \phi_{\pi^-} &= -\frac{1}{2} (\phi_{\pi^+} - \phi_{\pi^-}) - \frac{1}{\sqrt{2}} \phi_{\pi^0}, \\ \phi_{\pi^+} &= \frac{1}{2} (\phi_{\pi^+} - \phi_{\pi^-}) - \frac{1}{\sqrt{2}} \phi_{\pi^0}, \end{aligned} \quad (21)$$

while the light quark contribution to the electromagnetic current in Eq. (6), written in the rotated basis, takes the form

$$J_\mu(x) \rightarrow J'_\mu(x) \equiv \bar{J}_\mu(x) + J_\mu^{ib}(x), \quad (22)$$

where

$$\bar{J}_\mu(x) \equiv e \bar{q} \bar{\psi}'_\ell(x) \gamma_\mu \psi'_\ell(x) \quad (23)$$

$$J_\mu^{ib}(x) \equiv -e \Delta q \bar{q}'_\ell(x) \tau_1 \gamma_\mu \psi'_\ell(x) \quad (24)$$

with $\bar{q} = (q_u + q_d)/2$ and $\Delta q = (q_u - q_d)/2$. The IB component of the electromagnetic current J_μ^{ib} in Eq. (23) has an unconventional direction in flavor space, and induces a mixing between the u' and d' quarks.

Using Eq. (21) it is easily realized that the correlator $C_{\pi^+ \pi^-}(t) = \langle 0 | \phi_{\pi^+}(t) \phi_{\pi^-}^\dagger(0) | 0 \rangle$ which describes, in the rotated basis, the mixing between the positive and negative rotated pion fields, is related to the difference between the charged and neutral physical pion correlator via

$$C_{\pi^+ \pi^-}(t) = \frac{1}{2} (C_{\pi^0 \pi^0}(t) - C_{\pi^+ \pi^+}(t)). \quad (25)$$

The mixing is absent in the QCD isospin symmetric theory, and it is generated, in the RTM scheme, by a double insertion of the “flavor off-diagonal” component J_μ^{ib} of the rotated electromagnetic current, which is an $\mathcal{O}(\alpha_{\text{em}})$ effect. From this result it follows (see Ref. [16] for a detailed derivation), that the pion mass difference at $\mathcal{O}(\alpha_{\text{em}})$ can be expressed in this scheme as

$$\partial_t \left[\frac{\delta C_\pi^{\text{exch.}}(t) - \delta C_\pi^{\text{disc.}}(t)}{C_{\pi\pi}^{\text{isoQCD}}(t)} \right], \quad (26)$$

where we now also include explicitly the RC Z_A of the local current J_μ^{ib} , which in our TM setup renormalizes as the axial current for untwisted Wilson quarks. In the diagrams of Eq. (26), we show explicitly the sign of the Wilson parameter on each quark line, which gets always flipped

at the e.m. vertex where the u' quark turns into a d' quark and viceversa. Manifestly, in both exchange and disconnected diagrams, only the “rotated charged” isospin symmetric pion propagates, and the resulting correlation functions are affected by strongly reduced statistical errors. We refer to Ref. [16] for a statistical comparison between rotated and unrotated disconnected correlators as well as for a more detailed discussion about the renormalization properties and continuum limit of the correlation functions in Eq. (26). In the next section, we evaluate the charged/neutral pion mass splitting from the diagrams displayed in Eq. (26).

III. NUMERICAL RESULTS

As already mentioned, for this study we use the $N_f = 2 + 1 + 1$ ensembles of Wilson TM fermions generated by the ETMC by only considering the ensembles with $M_\pi L > 3.8$. With respect to Table I, we thus exclude from the final analysis the ensemble A40.24. This subset of ensembles correspond to pion masses in the range $M_\pi \in [250, 500]$ MeV and lattice spacings from $a \sim 0.089$ fm down to $a \sim 0.062$ fm. For the RC Z_A appearing in Eq. (26), we use the precise determination obtained from the method M_2 of Ref. [18], namely $Z_A = \{0.703(2), 0.714(2), 0.752(2)\}$ at $\beta = \{1.90, 1.95, 2.10\}$. To improve the precision on the disconnected diagram of Eq. (26), we devised a new numerical technique, tailored for quark disconnected diagrams, in which the photon propagator is evaluated exactly by working in momentum space, and therefore the statistical noise generated by its

stochastic representation is absent. The method, which is discussed in details in Appendix, combined with the benefit of the RTM scheme, allows us to obtain an $\mathcal{O}(1\%)$ statistical accuracy on the value of the disconnected diagram. As an example, we show in Fig. 1, for the ensemble D30.48 (see Table I), our determination of the effective slope $\delta m_{\text{eff}}(t)$ extracted from both the exchange and the disconnected diagram.

To reduce the sensitivity of the result to the uncertainties of the scale setting, we find it useful to consider the dimensionless ratio

$$R_\pi \equiv \frac{M_{\pi^+}^2 - M_{\pi^0}^2}{f_\pi^2} \approx \frac{2M_\pi}{f_\pi^2} (M_{\pi^+} - M_{\pi^0}), \quad (27)$$

where f_π is the pion decay constant, and M_π is the mass of the TM charged pion in isospin symmetric QCD. Aiming at a determination of the pion mass splitting with $\mathcal{O}(1\%)$ accuracy, it is however important to have control over the QCD exponentially suppressed finite size effects (FSEs) affecting both f_π and M_π , to which we apply the SU(2) ChPT (chiral perturbation theory) finite volume corrections at NNLO + resummation, i.e., the Colangelo-Dürr-Haefeli (CDH) formulas [23]. The latter depend on the knowledge of the four, scale dependent, SU(2) low-energy constants (LECs) $\bar{\ell}_1, \bar{\ell}_2, \bar{\ell}_3, \bar{\ell}_4$, for which in this work we adopt the values $\bar{\ell}_1(M_\pi^{\text{phys}}) = -0.4$, $\bar{\ell}_2(M_\pi^{\text{phys}}) = 4.3$, $\bar{\ell}_3(M_\pi^{\text{phys}}) = 3.2$, $\bar{\ell}_4(M_\pi^{\text{phys}}) = 4.4$. The size of such corrections is in all cases smaller than one percent.

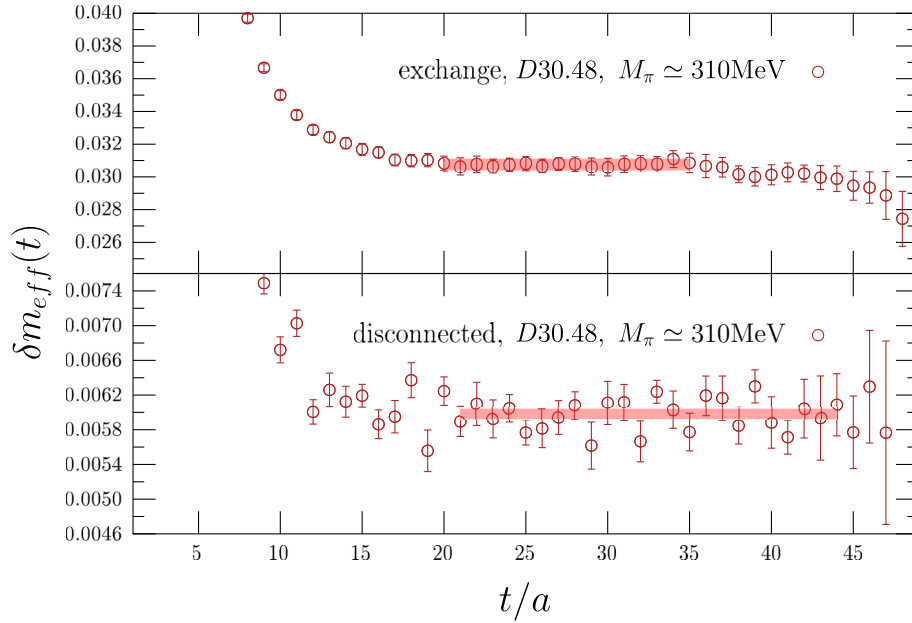


FIG. 1. Time dependence of the effective slope $\delta m_{\text{eff}}(t)$, in the case of the exchange (top) and of the disconnected (bottom) diagram, for the gauge ensemble D30.48. The horizontal bands indicate the result of a constant fit in the plateaux region where the ground state dominates.

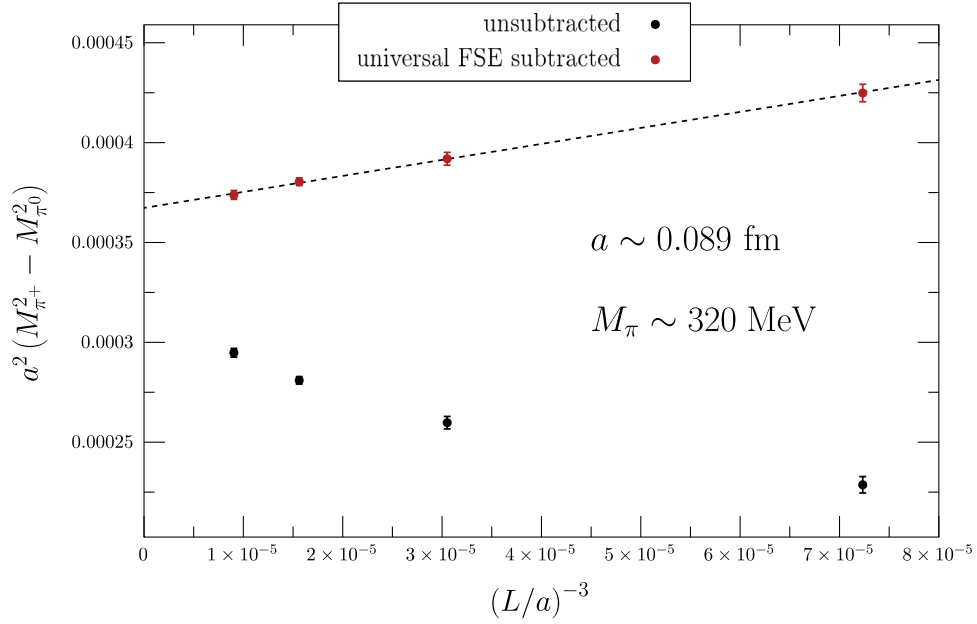


FIG. 2. The squared pion mass difference in the RTM scheme, for the ensembles of type A40.XX, which share a common value of the pion mass ($M_\pi \simeq 320$ MeV) and of the lattice spacing, but differ in the lattice size L . The black points represent the data in lattice units without any FSE correction, while the red ones are corrected subtracting the universal FSEs of Eq. (28). The dashed line is the result of a linear fit.

When a massless photon is put on a box, FSEs show up in QED observables as inverse powers of the spatial extent. The analysis of such finite volume corrections has been the subject of several studies (see Refs. [2,24]), where different infrared regularizations of QED have been considered. FSEs on hadron masses start at order $\mathcal{O}(L^{-1})$ and they are universal up to order $\mathcal{O}(L^{-2})$ included, i.e., their size depends solely on the charge, mass and spin of the hadron, but not on its internal structure. In the case of the QED_L which we use in this work, and for a pseudoscalar meson of electric charge Q and mass M_{PS} , the universal FSEs are given by

$$M_{\text{PS}}^2(L) - M_{\text{PS}}^2(\infty) = -Q^2 \alpha_{\text{em}} \frac{2\kappa}{L^2} \left(1 + \frac{1}{2} M_{\text{PS}} L\right), \quad (28)$$

where $\kappa = 2.837297$. Such corrections have been applied to our lattice data leaving residual structure-dependent (SD) $\mathcal{O}(L^{-3})$ FSEs. This is shown in Fig. 2 for the four ensembles of type A40.XX, which only differ in the spatial extent. For these ensembles, the residual FSEs are very well described by a $1/L^3$ term, and we do not see evidence of higher order $\mathcal{O}(L^{-4})$ FSEs within errors.

The SD FSEs arising in the QED_L regularization have been analyzed in Refs. [2,24–26]. In the nonrelativistic effective field theory approach developed in Ref. [24], the leading $\mathcal{O}(L^{-3})$ term is found to be proportional to the squared pion charge radius $\langle r^2 \rangle_{\pi^+}$ via

$$[M_{\pi^+}^2(L) - M_{\pi^+}^2(\infty)]^{(SD)} = \frac{e^2 M_\pi}{3 L^3} \langle r^2 \rangle_{\pi^+} + \mathcal{O}\left(\frac{1}{L^4}\right), \quad (29)$$

where $\langle r^2 \rangle_{\pi^+} = (0.672 \pm 0.008 \text{ fm})^2$. However, as discussed in Refs. [2,25,26], additional $\mathcal{O}(L^{-3})$ contributions, whose exact structure turns out to be difficult to determine theoretically, can be present in the full theory. At order $\mathcal{O}(L^{-4})$ QED-related FSEs starts to be present also for neutral pseudoscalar particles.

In Fig. 3 we show our determination of the R_π ratio, before and after removal of the universal FSEs of Eq. (28), as a function of the dimensionless ratio $M_\pi^2/(4\pi f_\pi)^2$. As the figure shows, the statistical accuracy is very good and in all cases of order of percent or smaller. The universal FSEs corrections are always sizable on our lattice volumes, approaching 45% at the largest simulated value of $M_\pi^2/(4\pi f_\pi)^2$.

According to the analysis of Refs. [27,28], the SU(3) ChPT prediction for the squared pion mass difference at NLO is given by

$$\begin{aligned} M_{\pi^+}^2 - M_{\pi^0}^2 = & e^2 f_0^2 C \left[1 - 4 \left(\frac{M_\pi}{4\pi f_0} \right)^2 \log \left(\frac{M_\pi}{4\pi f_0} \right)^2 \right. \\ & - 2 \left(\frac{M_K}{4\pi f_0} \right)^2 \log \left(\frac{M_K}{4\pi f_0} \right)^2 \left. \right] \\ & - 3e^2 f_0^2 \left(\frac{M_\pi}{4\pi f_0} \right)^2 \log \left(\frac{M_\pi}{4\pi f_0} \right)^2 \\ & + \mathcal{O}(M_\pi^2, M_K^2), \end{aligned} \quad (30)$$

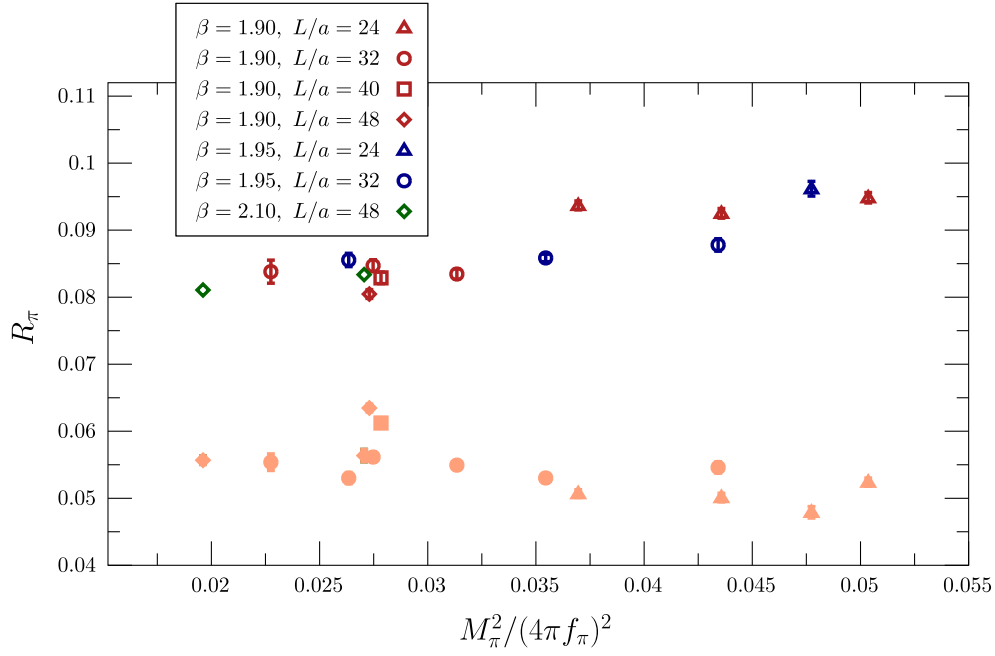


FIG. 3. Our results for the ratio R_π as a function of the dimensionless ratio $M_\pi^2/(4\pi f_\pi)^2$, determined in the RTM scheme and including the contribution of the disconnected diagram. The filled markers represent the data without any FSE correction, while the empty ones represent the result of the subtraction of the universal FSE using Eq. (28).

where f_0 is the pion decay constant in the chiral limit, and C is a LEC. Here and in the following two equations, we focus on the terms with the leading logarithmic dependence on the pseudoscalar light meson masses and denote by $\mathcal{O}(M_\pi^2, M_K^2)$ terms of first and higher order in the squared pion and kaon masses (involving further LECs), the presence of which will effectively be taken into account in the fit ansatz of Eq. (33). After inserting the SU(3) ChPT prediction for the pion decay constant at NLO [29]

$$f_\pi = f_0 \left[1 - 2 \left(\frac{M_\pi}{4\pi f_0} \right)^2 \log \left(\frac{M_\pi}{4\pi f_0} \right)^2 - \left(\frac{M_K}{4\pi f_0} \right)^2 \log \left(\frac{M_K}{4\pi f_0} \right)^2 \right] + \mathcal{O}(M_\pi^2, M_K^2), \quad (31)$$

we obtain for the ratio R_π the expression

$$R_\pi = 4e^2 C - 3e^2 \left(\frac{M_\pi}{4\pi f_0} \right)^2 \log \left(\frac{M_\pi}{4\pi f_0} \right)^2 + \mathcal{O}(M_\pi^2, M_K^2). \quad (32)$$

Notice that the chiral prediction for the ratio R_π is not affected, even in the SU(3) effective theory, by logarithmic corrections in the kaon mass, at NLO.

Inspired by the ChPT prediction of Eq. (32), and by the analysis of the SD FSEs of Refs. [24–26], we extrapolate the lattice data toward the physical pion mass and toward the continuum and infinite volume limit, employing the following ansatz for the ratio R_π

$$R_\pi^{\text{sub}}(\xi_\pi, a, L) = 4e^2 C - 3e^2 \xi_\pi \log \xi_\pi + e^2 A_1 \xi_\pi + e^2 A_2 \xi_\pi^2 + e^2 D a^2 + e^2 D_m \xi_\pi a^2 + e^2 K \frac{(4\pi)^2 \xi_\pi}{3M_\pi L^3} \langle r^2 \rangle_{\pi^+} \left(1 + \frac{F_4}{M_\pi L} \right) + e^2 F_a \frac{\xi_\pi a^2}{M_\pi L^3}, \quad (33)$$

where R_π^{sub} is the R_π ratio after the subtraction of the universal FSEs using Eq. (28), and $\xi_\pi \equiv M_\pi^2/(4\pi f_\pi)^2$ after applying the CDH corrections to M_π and f_π . In the previous expression C , A_1 , A_2 , D , D_m , K , F_a and F_4 are treated as free fitting parameters. In particular C and A_1 parameterize the ChPT expansion for R_π up to NLO, A_2 is an effective LEC at NNLO, while D and D_m take into account discretization effects. The constant K parametrizes deviations from the nonrelativistic prediction ($K = 1$) of Eq. (29) for the SD FSEs, the term proportional to a^2/L^3 corresponds to a FSE due to an heavy intermediate state of mass $\propto 1/a$ [25], and finally F_4 parametrizes higher order $\mathcal{O}(L^{-4})$ FSEs.

In Fig. 4, we show the result of the extrapolation obtained using the ansatz of Eq. (33), setting $A_2 = D = D_m = F_a = F_4 = 0$, which corresponds to our preferred fit. The quantity ΔM_π , which at the physical point gives the pion mass splitting, is defined as

$$\Delta M_\pi \equiv R_\pi \frac{(f_\pi^{\text{phys}})^2}{2M_\pi^{\text{phys}}}, \quad (34)$$

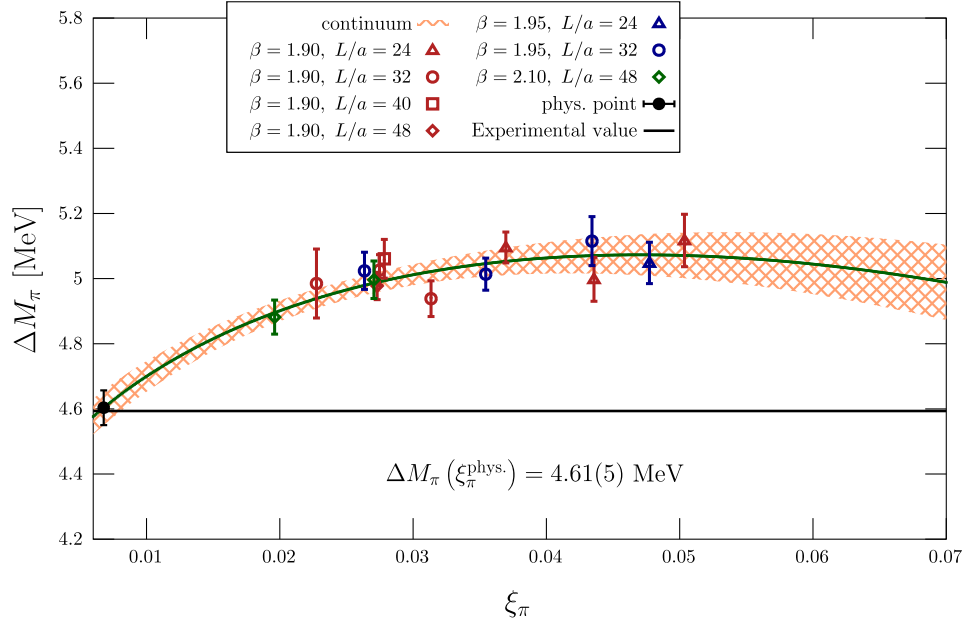


FIG. 4. Our results for ΔM_π as a function of the parameter ξ_π . The data points refer to our lattice estimate after the subtraction of both universal and SD FSEs. The solid lines represents, for each lattice spacing, the central value of the fitted curve in Eq. (33) obtained setting $A_2 = D = D_m = F_a = F_4 = 0$, and in the thermodynamic limit $L \rightarrow \infty$. The orange band shows the statistical uncertainty on ΔM_π after the continuum and infinite volume extrapolation. Finally, the black point corresponds to our determination at the physical point $\xi_\pi^{\text{phys}} \simeq 0.00678$ MeV.

with $M_\pi^{\text{phys}} = 134.977$ MeV and $f_\pi^{\text{phys}} = 130.4$ MeV. The reduced χ^2 of the fit is $\chi^2/\text{d.o.f.} \sim 1.8$ with 14 measures and 4 parameters. Notice the remarkable smallness of $\mathcal{O}(a^2)$ effects in our data. The inclusion of the fit parameter D to describe $\mathcal{O}(a^2)$ lattice artifacts does not improve the description of the data: the resulting $\chi^2/\text{d.o.f.}$ is 1.9 and the parameter D turns out to be consistent with zero within errors [$D = 0.04(10)$]. To estimate systematic errors, we perform a total of 24 fits, differing on whether the A_2 , the D , and the D_m fit parameters are included or not, and on the form of the SD FSEs for which we either include K or F_a as a free fit parameter (in this last case setting $K = 1$), or include the additional term $\propto F_4/L^4$ on top of the non-relativistic prediction $K = 1$, $F_a = 0$. The fit results are combined using the Akaike information criterion (AIC) [30], in which, to each fit, it is assigned a weight $w_i \propto \exp[-(\chi^2 + 2n_{\text{pars}})/2]$. Mean values and standard errors are then computed using [18,31,32]

$$\bar{x} = \sum_i w_i \bar{x}_i, \quad \sigma^2 = \sum_i w_i (\sigma_i^2 + (\bar{x}_i - \bar{x})^2), \quad (35)$$

where (\bar{x}_i, σ_i) is the mean value and the standard error obtained in the i th fit. Our final result for the pion mass splitting is

$$\begin{aligned} M_{\pi^+} - M_{\pi^0} &= 4.622(64)_{\text{stat}}(70)_{\text{syst1}} \text{ MeV} \\ &= 4.622(95) \text{ MeV}, \end{aligned} \quad (36)$$

which agrees very well with the experimental determination $[M_{\pi^+} - M_{\pi^0}]^{\text{exp}} = 4.5936(5)$ MeV, and with the result of a recent lattice determination [33] $M_{\pi^+} - M_{\pi^0} = 4.534(42)(43)$ MeV, in which the disconnected contribution has been computed as well.

IV. CONCLUSIONS

We have presented an analysis of the $\mathcal{O}(\alpha_{\text{em}})$ mass splitting $M_{\pi^+} - M_{\pi^0}$ between the charged and neutral pion, including the calculation of the disconnected diagram. We made use of the gauge configurations generated by the Extended Twisted Mass Collaboration with $N_f = 2 + 1 + 1$ dynamical quark flavors. The gauge ensembles considered corresponds to three different values of the lattice spacing $a \simeq 0.062, 0.082$ and 0.089 fm, pion masses in the range $M_\pi \simeq 250\text{--}450$ MeV, while the strange and charm quark masses are set in all ensembles to their physical value. We showed that a good accuracy in the determination of the disconnected diagram can be achieved by working in the *rotated twisted mass* (RTM) scheme, which have been shown to be particularly convenient for the evaluation of some QCD + QED mesonic observables based on the RM123 approach. We also developed a new numerical technique, tailored to quark-line disconnected diagrams, which does not rely on a stochastic representation of the photon propagator and that produced a further reduction of the statistical noise by more than one order of magnitude. After extrapolating to the continuum and infinite volume

limit, and at the physical point, we obtain a value for $M_{\pi^+} - M_{\pi^0}$ which perfectly agrees with the experimental result. With respect to our previous determination [14], we were able to reduce the uncertainty on the pion mass splitting by a factor ~ 3 , thanks to the use of the dimensionless ratio R_π , and its ChPT-based extrapolation analysis, and of larger lattice volumes.

ACKNOWLEDGMENTS

We thank C. Tarantino for useful discussions, and all members of ETMC for the most enjoyable collaboration. We acknowledge CINECA for the provision of CPU time under the specific initiative INFN-LQCD123 and IscrB_S-EPIC. F. S., G. G and S. S. are supported by the Italian Ministry of University and Research (MIUR) under Grant No. PRIN20172LNEEZ. F. S. and G. G are supported by INFN under GRANT73/CALAT.

APPENDIX: NUMERICAL METHODS FOR THE DISCONNECTED DIAGRAM

The disconnected contribution to the pion mass difference $M_{\pi^+} - M_{\pi^0}$, in the RTM basis, is encoded in the following Wick-contracted Green function of the isospin symmetric theory

$$G_{\mu\nu}^{(4)}(t-t', y, y') = \frac{1}{L^3} \sum_{\vec{x}, \vec{x}'} \langle 0 | T \left\{ \underbrace{\phi_{\pi^-}(\vec{x}, t) J_\mu^{ib}(y)}_{\text{diagram}} \cdot \underbrace{J_\nu^{ib}(y') \phi_{\pi^+}^\dagger(\vec{x}', t')}_{\text{diagram}} \right\} | 0 \rangle. \quad (\text{A1})$$

Equation (A1) can be in turn written as

$$G_{\mu\nu}^{(4)}(t-t', y, y') = 2e^2(\Delta q)^2 \cdot \langle G_\mu^{(2)}(t, y) G_\nu^{(2)}(t', y') \rangle_U, \quad (\text{A2})$$

where $\langle \cdot \rangle_U$ denotes the average over the SU(3) QCD gauge field, while

$$G_\mu^{(2)}(t, y) = \frac{1}{\sqrt{L^3}} \sum_{\vec{x}} \text{Tr} \{ S_\ell^+((\vec{x}, t), y) \gamma_\mu S_\ell^-(y, (\vec{x}, t)) \gamma_5 \}, \quad (\text{A3})$$

and Tr is meant over color and spin indices. In the previous equation, S_ℓ^\pm is the propagator of the two ‘‘flavor’’ components corresponding to Wilson parameters $r = \pm 1$ of the light quark isodoublet field ψ'_ℓ entering the RTM action in Eq. (17).

As illustrated in Sec. II B, the disconnected contribution to $M_{\pi^+} - M_{\pi^0}$, can be extracted from the large time

behavior of $\delta C_\pi^{\text{disc}}(t)/C_{\pi\pi}^{\text{isoQCD}}(t)$, where $C_{\pi\pi}^{\text{isoQCD}}(t)$ is the TM charged pion correlator

$$C_{\pi\pi}^{\text{isoQCD}}(t) = \frac{1}{\sqrt{L^3}} \sum_{\vec{x}} \langle 0 | T \{ \phi_{\pi^+}(\vec{x}, t) \phi_{\pi^+}^\dagger(0) \} | 0 \rangle, \quad (\text{A4})$$

and

$$\delta C_\pi^{\text{disc}}(t-t') = \frac{1}{2e^2(\Delta q)} \sum_{y, y'} G_{\mu\nu}^{(4)}(t, t', y, y') \Delta_{\mu\nu}(y, y'), \quad (\text{A5})$$

As usual, the QED corrections at order $\mathcal{O}(\alpha_{\text{em}})$ require the computation of the integrals over the two ends of the photon propagator [sum over y and y' in Eq. (A5)]. The explicit summation is, however, prohibitively costly on a large four dimensional lattice, as it scales like the square of the lattice volume $V = L^3 \cdot T$. To cope with this issue, in Ref. [14] a stochastic technique has been adopted to evaluate all connected diagrams arising at order $\mathcal{O}(\alpha_{\text{em}})$, and in this work we adopt the same strategy to compute the exchange diagram. The idea of the stochastic approach is to exploit the definition of the photon propagator in terms of the expectation value of the time ordered product of photon fields, i.e.,

$$\Delta_{\mu\nu}(y-y') = \langle A_\mu(y) A_\nu(y') \rangle_A. \quad (\text{A6})$$

One can then sample each mode of the photon field $A_\mu(y)$ from the local probability distribution in momentum space

$$P[\vec{A}(k)] d\vec{A}(k) \propto \exp(-A_\mu(k) \Delta_{\mu\nu}^{-1}(k) A_\nu(k)), \quad (\text{A7})$$

where in Feynman gauge $\Delta_{\mu\nu}^{-1}(k) = \delta_{\mu\nu}/\tilde{k}^2$, with

$$\tilde{k}^\nu = 2 \sin\left(\frac{k^\nu}{2}\right). \quad (\text{A8})$$

In our QED_L setup all the ‘‘spatial zero modes’’ $A_\mu(k^0, \vec{k} = 0)$ are removed. By drawing a sample $\{A_\mu^i\}_{i=1, \dots, n}$, the photon propagator can be estimated as

$$\Delta_{\mu\nu}(y-y') \simeq \frac{1}{n} \sum_{i=1}^n A_\mu^i(y) A_\nu^i(y'), \quad (\text{A9})$$

and the estimate becomes an exact equality in the infinite n limit. In this way, any observable of the form

$$\mathcal{O} = \sum_{y, y'} \langle \mathcal{O}_1^\mu(y) \cdot \mathcal{O}_2^\nu(y') \rangle_U \Delta_{\mu\nu}(y, y'), \quad (\text{A10})$$

can be split into two summations, each scaling as the lattice volume V , using

$$\mathcal{O} = \lim_{n \rightarrow \infty} \frac{1}{n} \sum_i \langle \mathcal{O}_1^{A^i} \cdot \mathcal{O}_2^{A^i} \rangle_U,$$

$$\mathcal{O}_j^{A^i} = \sum_y \mathcal{O}_j^{\mu}(y) A_{\mu}^i(y), \quad j = 1, 2. \quad (\text{A11})$$

We refer to the Appendix A of Ref. [14] for a detailed explanation on how this strategy can be implemented to efficiently evaluate the exchange diagram.

However, despite the stochastic technique proves itself useful in many occasions, the evaluation of the disconnected diagram turns out to be very noisy, requiring a too large value of n to get a clear signal. In this work we thus adopt a different strategy, specific to quark-line disconnected diagrams, that does not rely on a stochastic representation of the photon propagator, and allows to compute $\delta C_{\pi}^{\prime \text{disc}}$ in $\mathcal{O}(V \log V)$ time.

Starting from Eq. (A3), we define

$$\tilde{B}_{\nu}(t, y') \stackrel{\text{def}}{=} \sum_y G_{\mu}^{(2)}(t, y) \Delta_{\mu\nu}(y - y'), \quad (\text{A12})$$

which is nothing but the convolution $G_{\mu}^{(2)}(t) * \Delta_{\mu\nu}$. In Fourier space we thus have

$$\tilde{B}_{\nu}(t, k) = G_{\mu}^{(2)}(t, k) \Delta_{\mu\nu}(k) = G_{\nu}^{(2)}(t, k) / \tilde{k}^2, \quad (\text{A13})$$

where on a $L^3 \times T$ torus and within the QED_L theory we considered, the set of allowed momenta k is given by

$$k = 2\pi \left(\frac{n_0}{T}, \frac{n_1}{L}, \frac{n_2}{L}, \frac{n_3}{L} \right), \quad (\text{A14})$$

$$n_0 \in \{0, \dots, T-1\}, \quad (\text{A15})$$

$$n_{i=1,2,3} \in \{1, \dots, L-1\}. \quad (\text{A16})$$

The quantity $G_{\mu}^{(2)}(t, k)$ can be computed from $G_{\mu}^{(2)}(t, x)$ using fast Fourier transform (FFT) methods in $\mathcal{O}(V \log V)$ time. Moreover, transforming back from $\tilde{B}(t, k)$ to $\tilde{B}(t, y')$ via

$$\tilde{B}_{\nu}(t, y') = \sum_k e^{-iky'} \tilde{B}_{\nu}(t, k), \quad (\text{A17})$$

can be done within a similar machine time. The disconnected diagram $\delta C_{\pi}^{\prime \text{disc}}(t' - t)$ is then obtained from the product between the ‘‘bubble diagram’’ $G_{\mu}^{(2)}(t', y')$ and $\tilde{B}_{\mu}(t, y')$ via

$$\delta C_{\pi}^{\prime \text{disc}}(t' - t) = \sum_{y'} \tilde{B}_{\nu}(t, y') G_{\nu}^{(2)}(t', y'), \quad (\text{A18})$$

which requires $\mathcal{O}(V)$ operations, and the overall complexity of the computation is thus of order $\mathcal{O}(V \log V)$.

Concerning the bubble diagram $G_{\mu}^{(2)}(t, y)$, for each gauge configuration its value can be estimated through a

single inversion of the lattice Dirac operator as in the case of the pion correlator of the isospin symmetric theory. As is standard practice, the inversion is performed stochastically using a certain number $N_s(t)$ of random sources. This induces, as usual, an uncertainty on $G_{\mu}^{(2)}(t, y)$ that scales as $(N_s(t))^{-1/2}$. The noise induced by the use of the stochastic method on $\delta C_{\pi}^{\prime \text{disc}}(\Delta t = t' - t)$ at a given Δt , depends instead on two factors. The first one is clearly the total number $N(\Delta t)$ of stochastic sources separated by a time distance Δt , i.e.,

$$N(\Delta t) = \sum_{t=0}^{T-1} N_s(t) \cdot N_s((t + \Delta t) \bmod T). \quad (\text{A19})$$

Indeed, defining $\delta C_{\pi}^{\prime \text{disc}}(\Delta t, t_i, t'_j)$ to be the estimate of $\delta C_{\pi}^{\prime \text{disc}}(\Delta t)$ obtained considering only the i th random source at time t and the j th random source at time $t' = (t + \Delta t) \bmod T$, the value of $\delta C_{\pi}^{\prime \text{disc}}(\Delta t)$ is estimated through

$$\delta C_{\pi}^{\prime \text{disc}}(\Delta t) \sim \frac{1}{N(\Delta t)} \sum_{t=0}^{T-1} \sum_{i=1}^{N_s(t)} \sum_{j=1}^{N_s(t')} \delta C_{\pi}^{\prime \text{disc}}(\Delta t, t_i, t'_j). \quad (\text{A20})$$

However, the statistical uncertainty on $\delta C_{\pi}^{\prime \text{disc}}(\Delta t)$ does not scale exactly as $(N(\Delta t))^{-1/2}$ since a given random source appears in general many times in the sum of Eq. (A20), inducing a correlation between the various terms. Thus, understanding how the uncertainty on $\delta C_{\pi}^{\prime \text{disc}}(\Delta t)$ behaves depending on the choice of the $N_s(t)$ is a nontrivial problem. Given a fixed number of sources $N_s^{\text{tot}} = \sum_{t=0}^{T-1} N_s(t)$, one would like to find the optimal way of

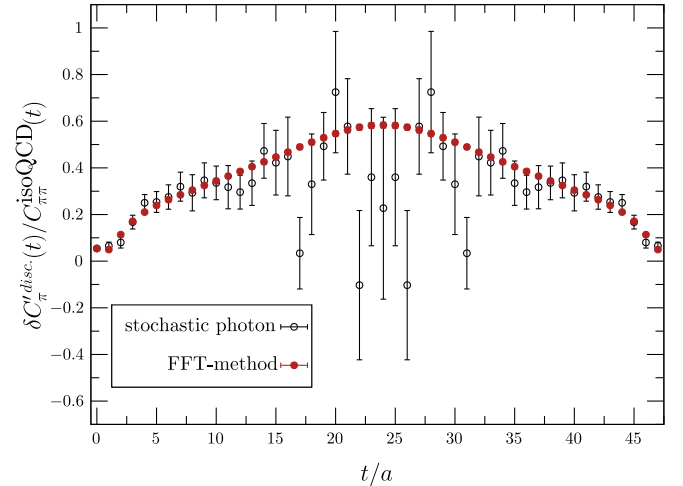


FIG. 5. Ratio of correlators $\delta C_{\pi}^{\prime \text{disc}}(t) / C_{\pi\pi}^{\text{isoQCD}}(t)$ computed using the FFT-based method (solid points), and the stochastic one in which the photon field A_{μ} is sampled (empty points). The two datasets correspond to simulations on a $24^3 \times 48$ lattice at $\beta = 1.90$ having a similar numerical cost.

distributing the N_s^{tot} sources along the time direction, in such a way that the signal of $\delta C_\pi^{\prime\text{disc}}(\Delta t)$ is optimized in a given interval $\Delta t \in [t_{\text{min}}, t_{\text{max}}]$ where one expects the ground-state to be dominant. However, after performing preliminary tests using $N_s^{\text{tot}} = T$, we found that the uniform distribution $N_s(t) = 1$, produces the smallest errors among various choices of the distribution of the random sources. The results presented in Sec. III have been obtained employing $N_s(t) = 1$ for all simulation points.

Finally, we show in Fig. 5 a comparison between the ratio of correlators $\delta C_\pi^{\prime\text{disc}}(t)/C_{\pi\pi}^{\text{isoQCD}}(t)$ computed using both the FFT-based and the stochastic method. The comparison is performed at approximately equal total machine time, on a $24^3 \times 48$ lattice at $\beta = 1.90$ and with a pion mass $M_\pi \sim 320$ MeV. As it can be seen from the figure the improvement is dramatic, with the precision on $\delta C_\pi^{\prime\text{disc}}(t)/C_{\pi\pi}^{\text{isoQCD}}(t)$ improving by a factor 10–20.

-
- [1] Y. Aoki, T. Blum, G. Colangelo, S. Collins, M. Della Morte, P. Dimopoulos, S. Dürer, X. Feng, H. Fukaya, M. Golterman *et al.*, FLAG review 2021, [arXiv:2111.09849](https://arxiv.org/abs/2111.09849).
- [2] S. Borsanyi, S. Durr, Z. Fodor, C. Hoelbling, S. D. Katz, S. Krieg, L. Lellouch, T. Lippert, A. Portelli, K. K. Szabo *et al.*, Ab initio calculation of the neutron-proton mass difference, *Science* **347**, 1452 (2015).
- [3] P. Boyle, V. Gülpers, J. Harrison, A. Jüttner, C. Lehner, A. Portelli, and C. T. Sachrajda, Isospin breaking corrections to meson masses and the hadronic vacuum polarization: A comparative study, *J. High Energy Phys.* **09** (2017) 153.
- [4] M. Hansen, B. Lucini, A. Patella, and N. Tantalo, Gauge invariant determination of charged hadron masses, *J. High Energy Phys.* **05** (2018) 146.
- [5] S. Basak *et al.* (MILC Collaboration), Lattice computation of the electromagnetic contributions to kaon and pion masses, *Phys. Rev. D* **99**, 034503 (2019).
- [6] G. M. de Divitiis *et al.* (RM123 Collaboration), Isospin breaking effects due to the up-down mass difference in lattice QCD, *J. High Energy Phys.* **04** (2012) 124.
- [7] G. M. de Divitiis, R. Frezzotti, V. Lubicz, G. Martinelli, R. Petronzio, G. C. Rossi, F. Sanfilippo, S. Simula, and N. Tantalo (RM123 Collaboration), Leading isospin breaking effects on the lattice, *Phys. Rev. D* **87**, 114505 (2013).
- [8] D. Giusti, V. Lubicz, C. Tarantino, G. Martinelli, C. T. Sachrajda, F. Sanfilippo, S. Simula, and N. Tantalo (RM123 Collaboration), First Lattice Calculation of the QED Corrections to Leptonic Decay Rates, *Phys. Rev. Lett.* **120**, 072001 (2018).
- [9] M. Di Carlo, G. Martinelli, D. Giusti, V. Lubicz, C. T. Sachrajda, F. Sanfilippo, S. Simula, and N. Tantalo (RM123 Collaboration), Light-meson leptonic decay rates in lattice QCD + QED, *Phys. Rev. D* **100**, 034514 (2019).
- [10] A. Desiderio *et al.* (RM123 Collaboration), First lattice calculation of radiative leptonic decay rates of pseudoscalar mesons, *Phys. Rev. D* **103**, 014502 (2021).
- [11] D. Giusti, V. Lubicz, G. Martinelli, F. Sanfilippo, and S. Simula (RM123 Collaboration), Strange and charm HVP contributions to the muon ($g - 2$) including QED corrections with twisted-mass fermions, *J. High Energy Phys.* **10** (2017) 157.
- [12] D. Giusti, V. Lubicz, G. Martinelli, F. Sanfilippo, and S. Simula (RM123 Collaboration), Electromagnetic and strong isospin-breaking corrections to the muon $g - 2$ from Lattice QCD + QED, *Phys. Rev. D* **99**, 114502 (2019).
- [13] S. Borsanyi, Z. Fodor, J. N. Guenther, C. Hoelbling, S. D. Katz, L. Lellouch, T. Lippert, K. Miura, L. Parato, K. K. Szabo *et al.*, Leading hadronic contribution to the muon magnetic moment from lattice QCD, *Nature (London)* **593**, 51 (2021).
- [14] D. Giusti, V. Lubicz, C. Tarantino, G. Martinelli, F. Sanfilippo, S. Simula, and N. Tantalo (RM123 Collaboration), Leading isospin-breaking corrections to pion, kaon and charmed-meson masses with Twisted-Mass fermions, *Phys. Rev. D* **95**, 114504 (2017).
- [15] R. F. Dashen, Chiral SU(3) \otimes SU(3) as a symmetry of the strong interactions, *Phys. Rev.* **183**, 1245 (1969).
- [16] R. Frezzotti, G. Gagliardi, V. Lubicz, F. Sanfilippo, and S. Simula, Rotated twisted-mass: A convenient regularization scheme for isospin breaking QCD and QED lattice calculations, *Eur. Phys. J. A* **57**, 282 (2021).
- [17] R. Baron *et al.* (ETM Collaboration), Light hadrons from lattice QCD with light (u, d), strange and charm dynamical quarks, *J. High Energy Phys.* **06** (2010) 111.
- [18] N. Carrasco *et al.* (ETM Collaboration), Up, down, strange and charm quark masses with $N_f = 2 + 1 + 1$ twisted mass lattice QCD, *Nucl. Phys.* **B887**, 19 (2014).
- [19] P. A. Zyla *et al.* (Particle Data Group), Review of particle physics, *Prog. Theor. Exp. Phys.* **2020**, 083C01 (2020).
- [20] R. Frezzotti and G. C. Rossi, Chirally improving Wilson fermions I. O(a) improvement, *J. High Energy Phys.* **08** (2004) 007.
- [21] Z. R. Kordov *et al.* (CSSM/QCDSF/UKQCD Collaborations), State mixing and masses of the π^0 , η and η' mesons from $n_f = 1 + 1 + 1$ lattice QCD + QED, *Phys. Rev. D* **104**, 114514 (2021).
- [22] R. Frezzotti and G. C. Rossi, Chirally improving Wilson fermions. II. Four-quark operators, *J. High Energy Phys.* **10** (2004) 070.
- [23] G. Colangelo, S. Durr, and C. Haefeli, Finite volume effects for meson masses and decay constants, *Nucl. Phys.* **B721**, 136 (2005).
- [24] Z. Davoudi and M. J. Savage, Finite-volume electromagnetic corrections to the masses of mesons, baryons and nuclei, *Phys. Rev. D* **90**, 054503 (2014).

- [25] N. Tantalo, V. Lubicz, G. Martinelli, C.T. Sachrajda, F. Sanfilippo, and S. Simula, Electromagnetic corrections to leptonic decay rates of charged pseudoscalar mesons: Finite-volume effects, Proc. Sci., LATTICE2016 (2016) 300 [arXiv:1612.00199].
- [26] M. Di Carlo, M. T. Hansen, N. Hermansson-Truedsson, and A. Portelli, Relativistic, model-independent determination of electromagnetic finite-size effects beyond the point-like approximation, Phys. Rev. D **105**, 074509 (2022).
- [27] R. Urech, Virtual photons in chiral perturbation theory, Nucl. Phys. **B433**, 234 (1995).
- [28] M. Hayakawa and S. Uno, QED in finite volume and finite size scaling effect on electromagnetic properties of hadrons, Prog. Theor. Phys. **120**, 413 (2008).
- [29] J. Gasser and H. Leutwyler, Chiral perturbation theory: Expansions in the mass of the strange quark, Nucl. Phys. **B250**, 465 (1985).
- [30] H. Akaike, A new look at the statistical model identification, IEEE Trans. Autom. Control **19**, 716 (1974).
- [31] C. Alexandrou *et al.* (ETM Collaboration), Quark masses using twisted-mass fermion gauge ensembles, Phys. Rev. D **104**, 074515 (2021).
- [32] W.I. Jay and E. T. Neil, Bayesian model averaging for analysis of lattice field theory results, Phys. Rev. D **103**, 114502 (2021).
- [33] X. Feng, L. Jin, and M. J. Riberdy, Lattice QCD Calculation of the Pion Mass Splitting, Phys. Rev. Lett. **128**, 052003 (2022).